Electronic Supplementary Material (ESI) for Physical Chemistry Chemical Physics.

Electronic Supplementary Information - How does α_1Histidine102 affect the binding of modulators to $\alpha_1\beta_2\gamma_2$ $GABA_A$ receptors? Molecular insights from *in silico* experiments.

María Julia Amundarain, Ernesto Raul Caffarena and Marcelo Daniel Costabel

Methods

Development of the model and the complex with diazepam and flumazenil

To obtain a model of the $\alpha_1\beta_2\gamma_2$ $GABA_AR$ based on the β3 homopentamer[1] (PDB ID: 4COF) we created multiple alignments with PROMALS[2], HHPRED[3] and Swiss Model[4,5]. We compared the results from the three web-servers and altered the consensus manually in order to agree with experimental data, as highlighted by Bergmann et al.[6].
We used the Automodel class of Modeller 9.14[7] and the highest level of refinement to generate 500 initial models, which were then ranked according to Modeller scores and the best model was determined as the one with the largest percentage of residues in the favoured regions of the Ramachandran plot. Further analysis with ProSa z-score[8], Q-mean score[9] and PROCHECK[10] were also taken into account. The chosen model was refined with Coot[11] to optimize rotamers and side-chain interactions, and PROPKA[12,13] together with PDB2PQR[14,15] webserver were employed to assign protonation states and optimize hydrogen-bond networks.

The poses of the ligands in complex with the receptor and were acquired from docking with AutoDock Vina[16], a selection protocol based on indexes of precision and recall based on experimental information available, and subsequent refining molecular dynamics simulations of the whole receptor embedded in a POPC membrane as explained elsewhere[17].

Parameterization of the ligands:

GAFF force field was used to describe the atoms of the ligands. The parameters of the different atom types are specified in the original article by Wang et. al.[18].

Table S1: Atom types and partial charges for diazepam

Atom Name	Atom Type	Partial Charge
"H8"	"ha"	0.153000
"C8"	"ca"	-0.091000
"C9"	"ca"	-0.008600
"Cl"	"cl"	-0.081400
"C7"	"ca"	-0.162000
"H7"	"ha"	0.148000
"C6"	"ca"	0.083600
"C13"	"ca"	-0.201900
"C5"	"ce"	0.537500
"N15"	"n2"	-0.574900
"C17"	"c3"	0.038800
"C18"	"c"	0.688500
"O1"	"o"	-0.606500
"N2"	"n"	-0.384000
"C20"	"c3"	0.072300
"C12"	"ca"	-0.144900
"C4"	"ca"	-0.096500
"H4"	"ha"	0.144000
"C11"	"ca"	-0.096500
"H11"	"ha"	0.144000
"C1"	"ca"	-0.137000
"H1"	"ha"	0.136000
"C2"	"ca"	-0.115000
"H2"	"ha"	0.134000
"C3"	"ca"	-0.137000
"H3"	"ha"	0.136000
"C14"	"ca"	-0.076000
"H14"	"ha"	0.163000
"H172"	"h1"	0.088700
"H173"	"h1"	0.088700
"H201"	"h1"	0.053367
"H202"	"h1"	0.053367
"H203"	"h1"	0.053367

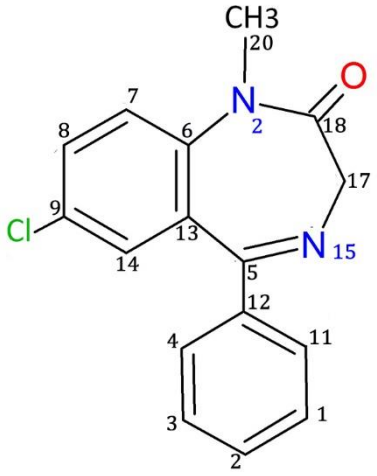

Table S2: Atom types and partial charges for flumazenil

Atom Name	Atom Type	Partial Charge
"C1"	"c3"	-0.101100
"C2"	"c3"	0.140400
"O3"	"os"	-0.461900
"C4"	"c"	0.575600
"O5"	"o"	-0.510000
"C6"	"cc"	0.278800
"C7"	"cd"	-0.145900
"C8"	"c3"	0.148300
"N9"	"n"	-0.457800
"C10"	"c"	0.704100
"O11"	"o"	-0.618500
"C12"	"ca"	-0.109600
"C13"	"ca"	0.015800
"N14"	"na"	-0.140000

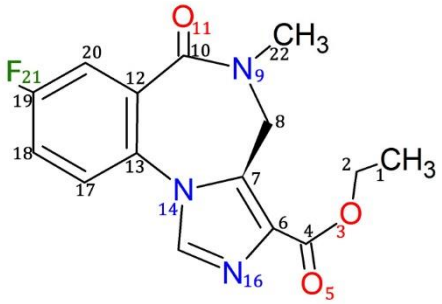

"C15"	"cd"	0.412400
"N16"	"nc"	-0.603000
"C17"	"ca"	-0.123000
"C18"	"ca"	-0.133000
"C19"	"ca"	0.123900
"C20"	"ca"	-0.107000
"C22"	"c3"	0.069300
"F21"	"f"	-0.126900
"H20"	"h1"	0.053700
"H101"	"hc"	0.047033
"H202"	"h1"	0.055700
"H801"	"h1"	0.091200
"H221"	"h5"	0.075100
"H15"	"ha"	0.154000
"H17"	"ha"	0.162000
"H18"	"ha"	0.179000
"H222"	"h1"	0.053700
"H102"	"hc"	0.047033
"H201"	"h1"	0.055700
"H802"	"h1"	0.091200
"H223"	"h1"	0.053700
"H103"	"hc"	0.047033

AM1-BCC is an atomic charge model for organic molecules in polar media. AM1 are atomic charges based on the occupancies of the atomic orbitals [19], and BCC stands for Bond Charge Corrections, that are applied to the AM1 atomic charges to correctly emulate the HF/6-31G* electrostatic potential.

Results

Table S3: pKa values obtained from three different webservers using PARSE force field.

Method	pKa ±1
PROPKA	3.7
DelPhi	6.2
MCCE	4.1

Classic MD simulations of diazepam-containing systems:

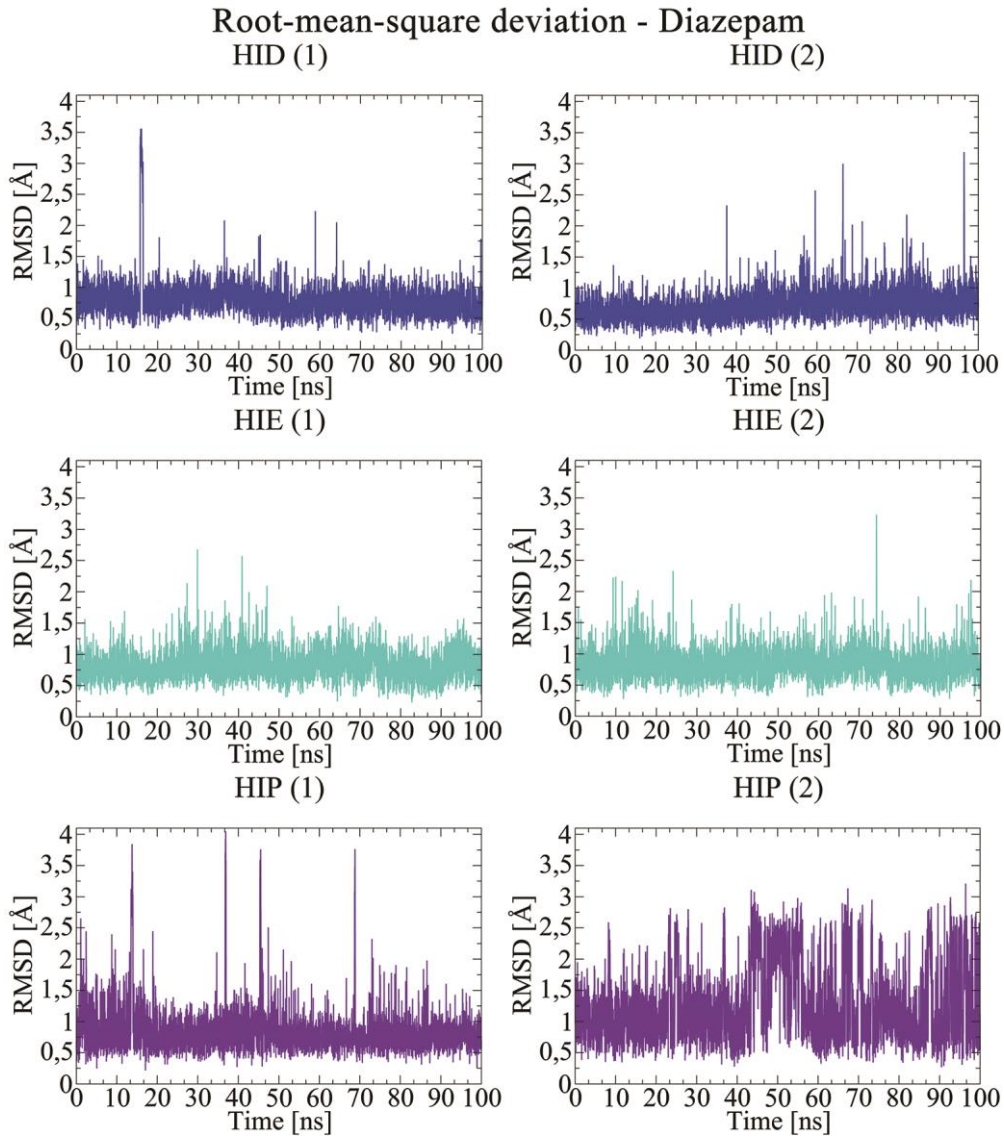

Figure S1: Root-mean-square deviation (RMSD) values for diazepam, fitted on the backbone of the protein of the diazepam-containing simulations.

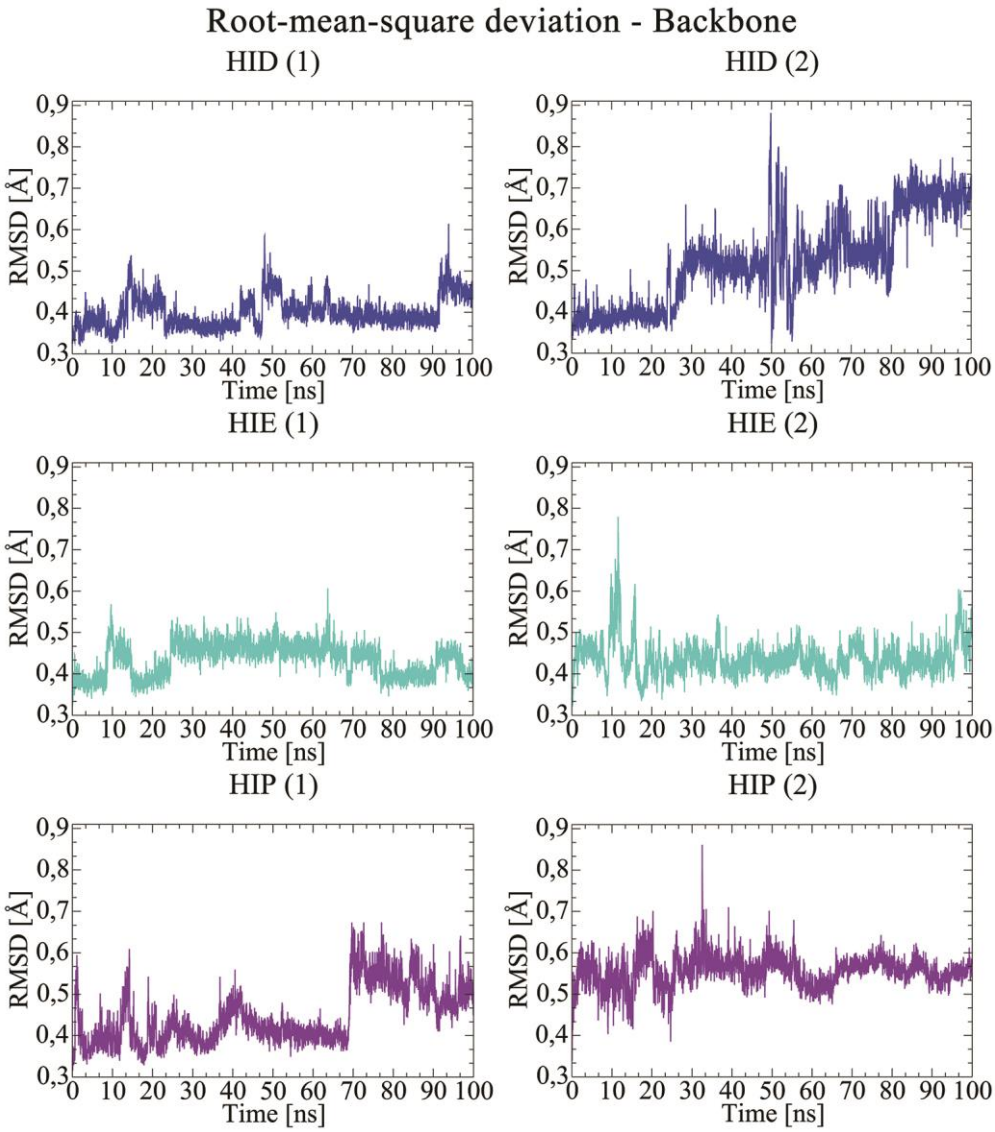

Figure S2: Root-mean-square deviation (RMSD) values for the backbone of the diazepam-containing simulations.

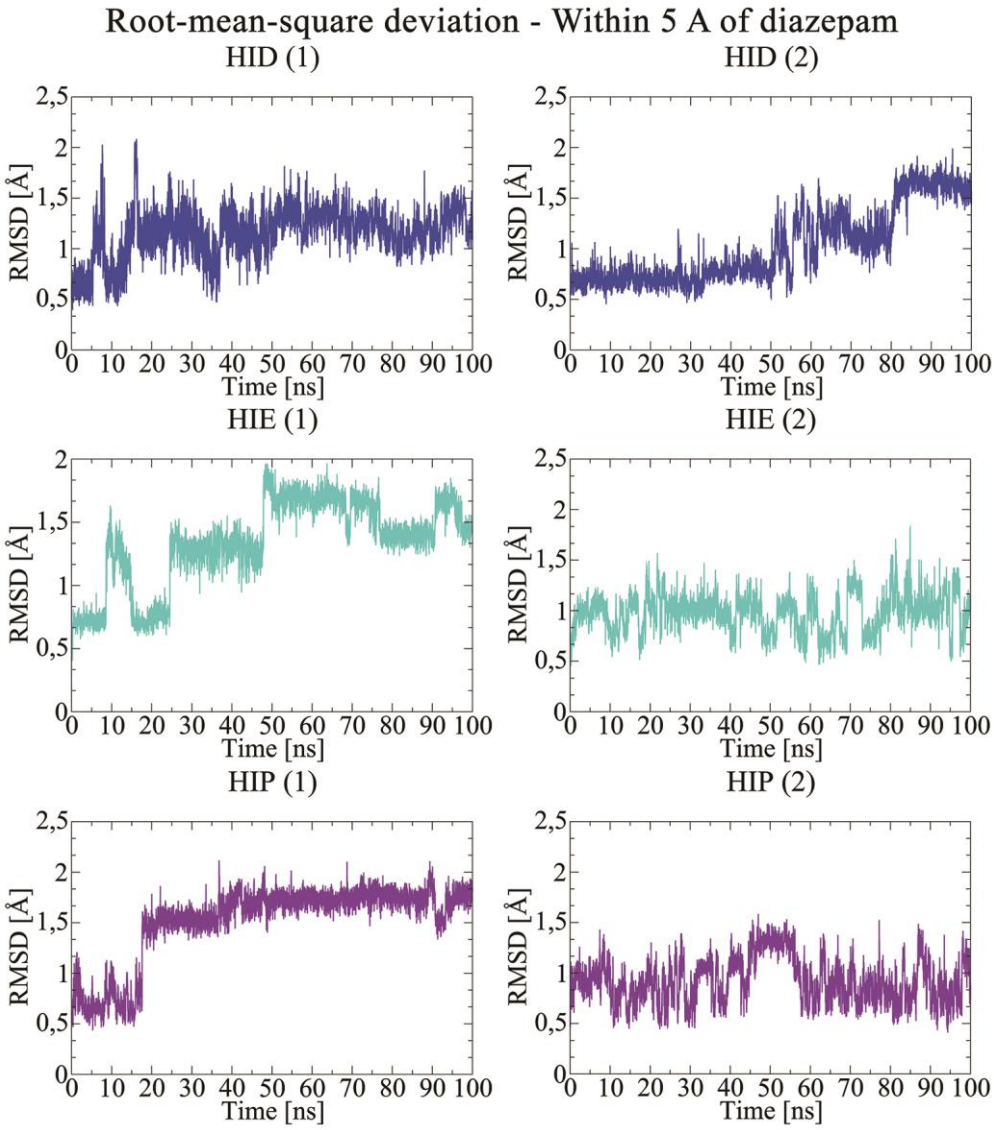

Figure S3: Root-mean-square deviation (RMSD) values of the protein residues that are within 5 Å of diazepam, fitted on the backbone of the protein of the diazepam-containing simulations.

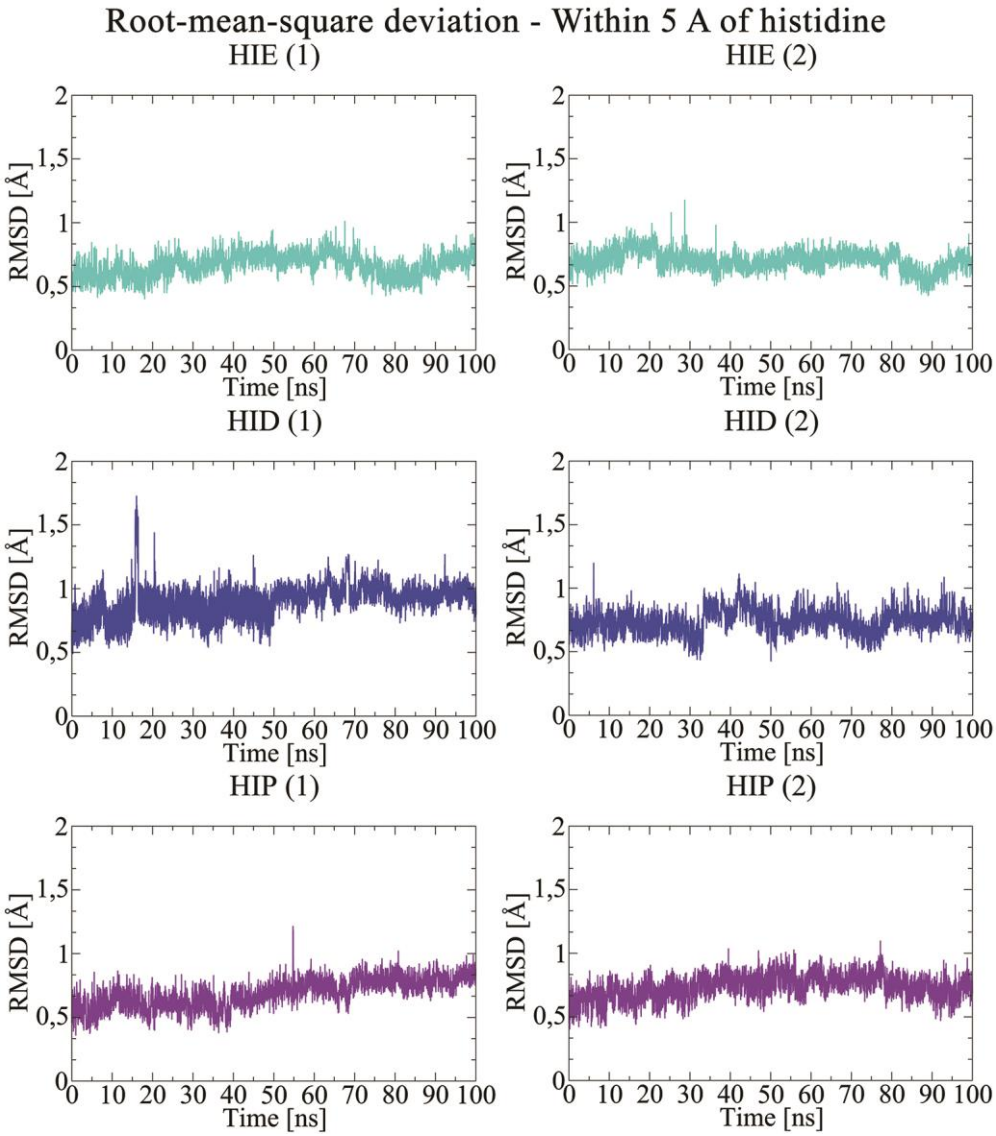

Figure S4: Root-mean-square deviation (RMSD) values of the protein residues that are within 5 Å of histidine, fitted on the backbone of the protein of the diazepam-containing simulations.

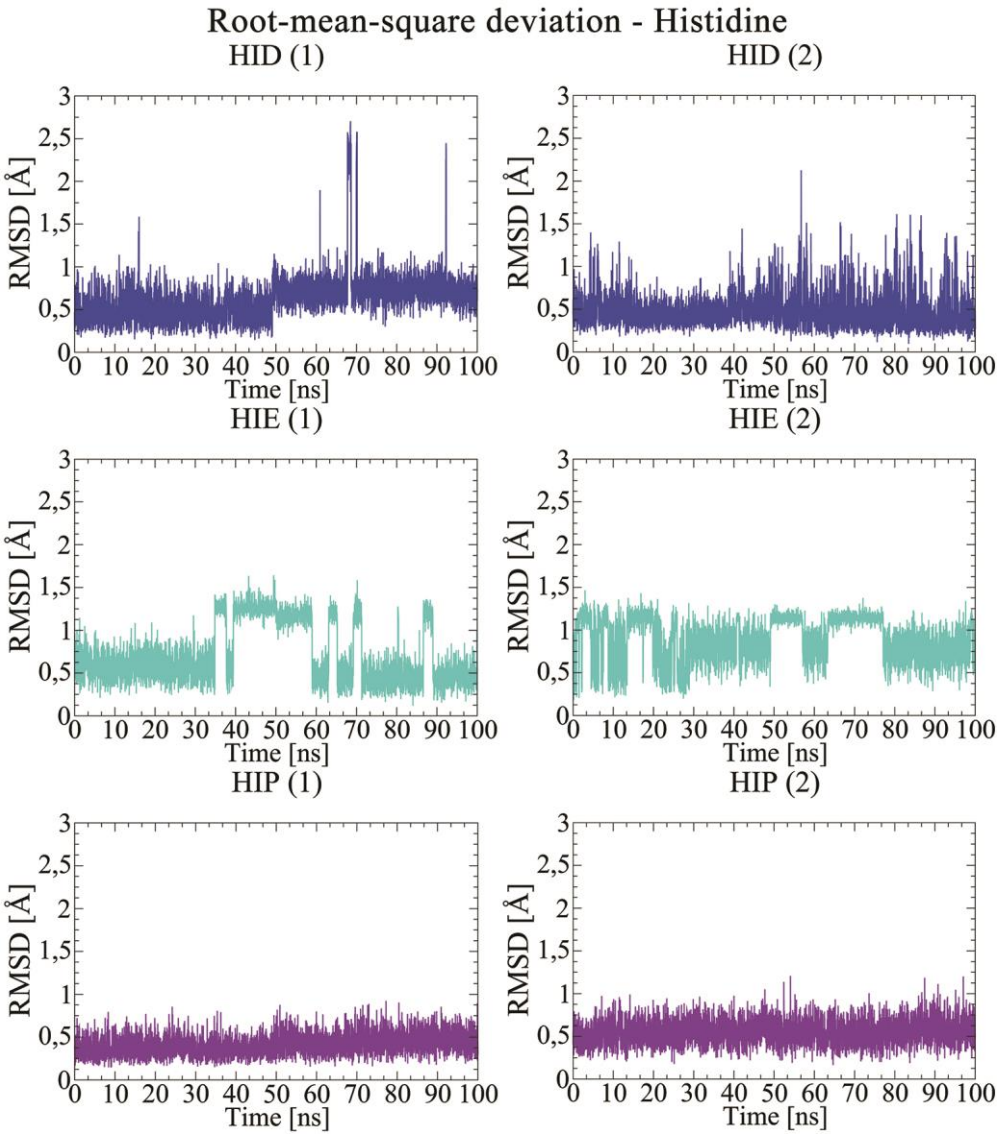

Figure S5: Root-mean-square deviation (RMSD) values for histidine, fitted on the backbone of the protein of the diazepam-containing simulations.

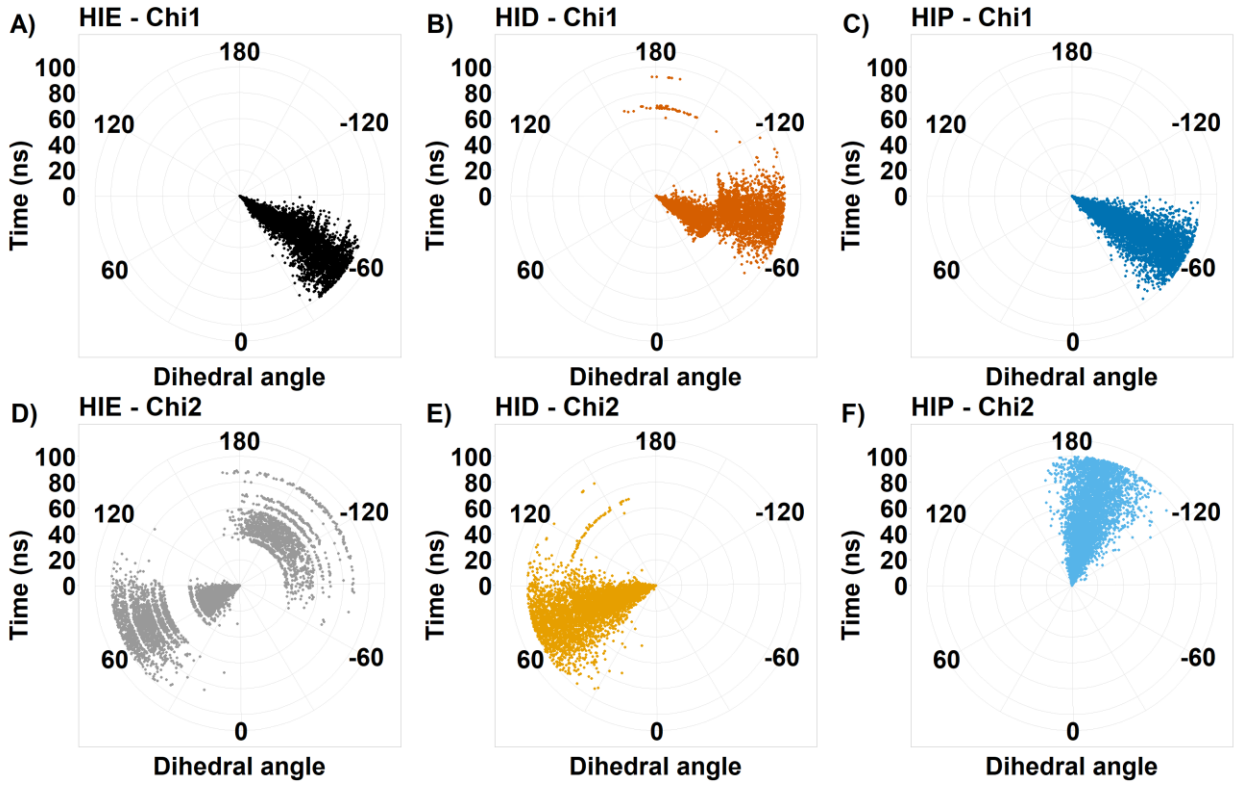

Figure S6: Dihedral distributions for the second set of simulations of diazepam in complex with the receptor. The dihedrals adopted by histidine are similar to those obtained in the other set of trajectories.

Classic MD simulations of flumazenil-containing systems:

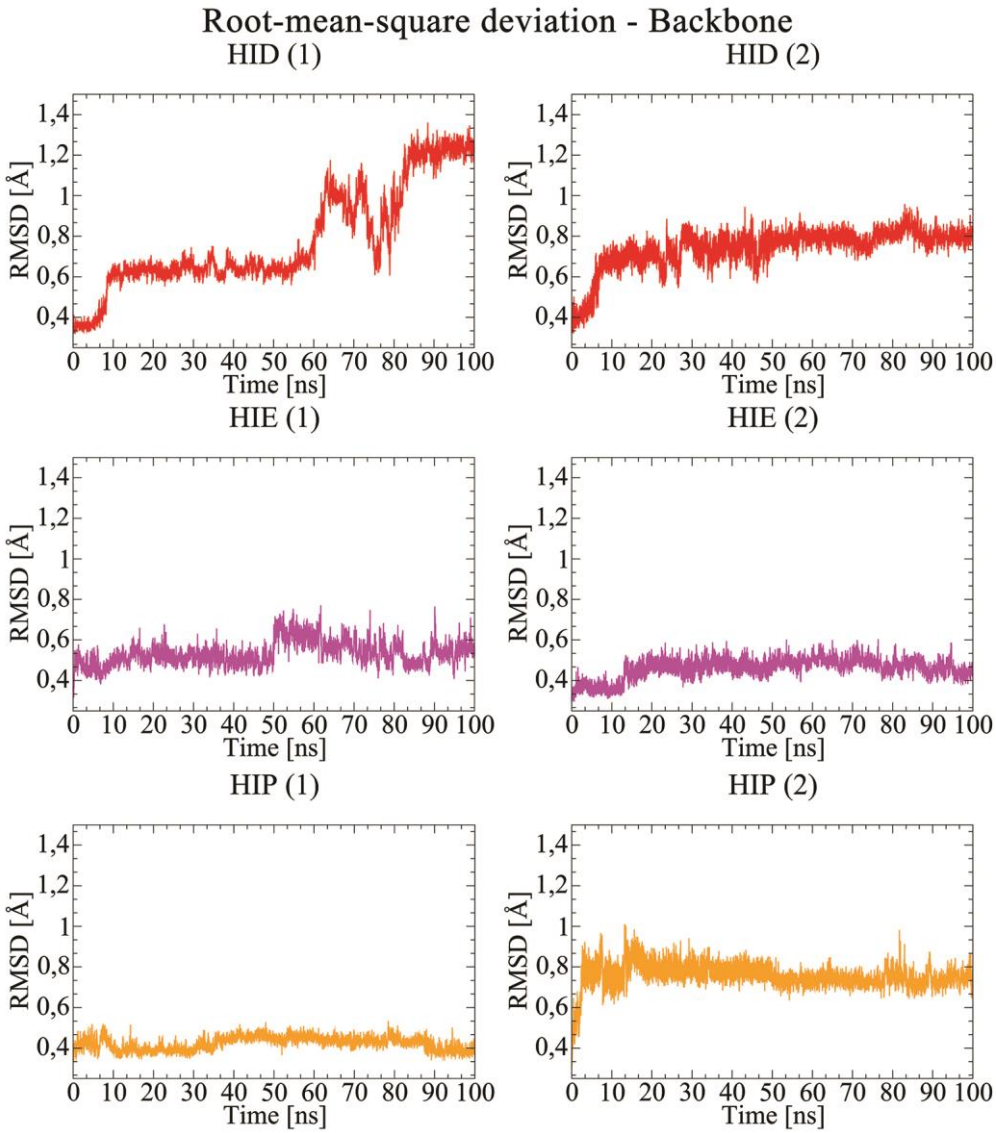

Figure S7: Root-mean-square deviation (RMSD) values for the backbone, fitted on the backbone of the protein of the flumazenil-containing simulations.

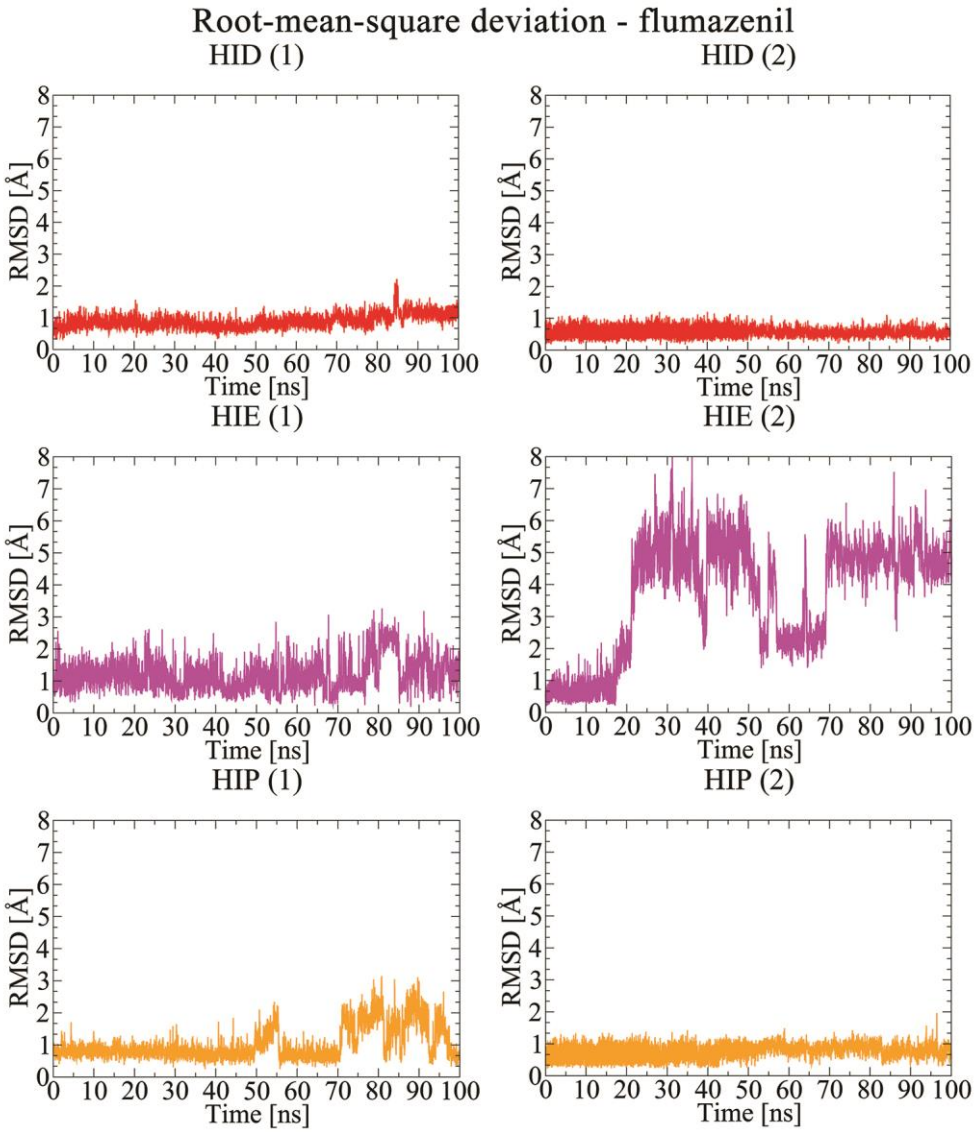

Figure S8: Root-mean-square deviation (RMSD) values for flumazenil, fitted on the backbone of the protein of the flumazenil-containing simulations.

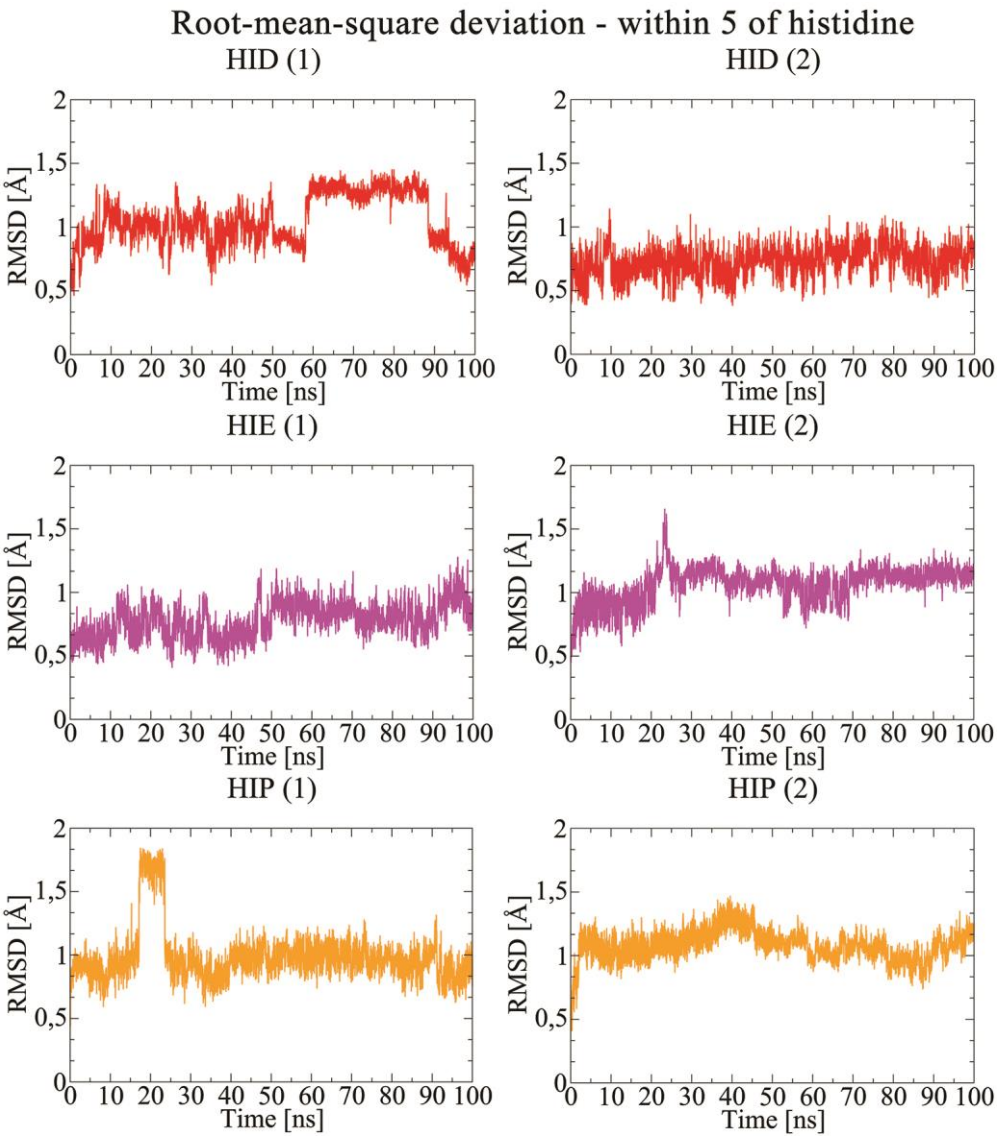

Figure S9: Root-mean-square deviation (RMSD) values of the protein residues that are within 5 Å of histidine, fitted on the backbone of the protein of the flumazenil-containing simulations.

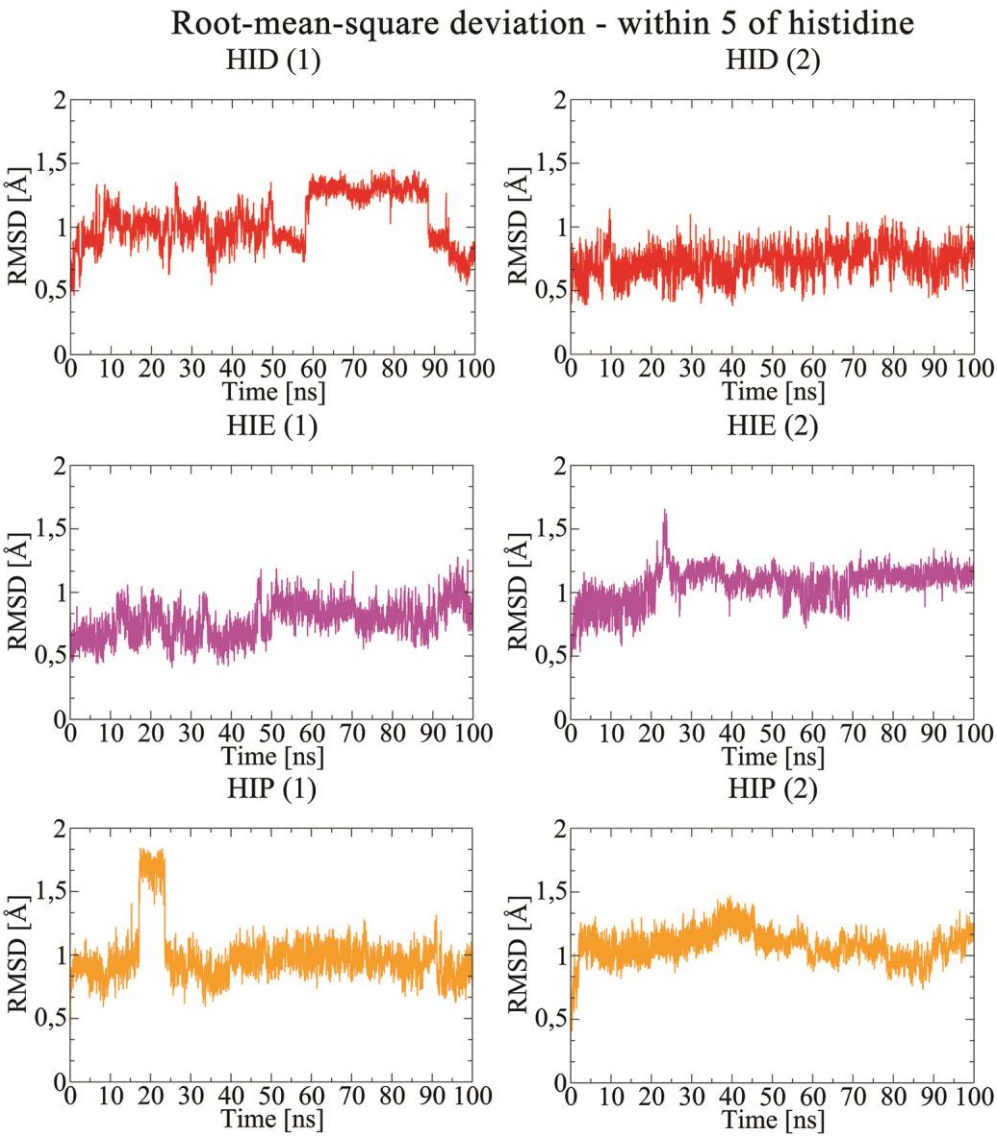

Figure S10: Root-mean-square deviation (RMSD) values of the protein residues that are within 5 Å of flumazenil, fitted on the backbone of the protein of the flumazenil-containing simulations.

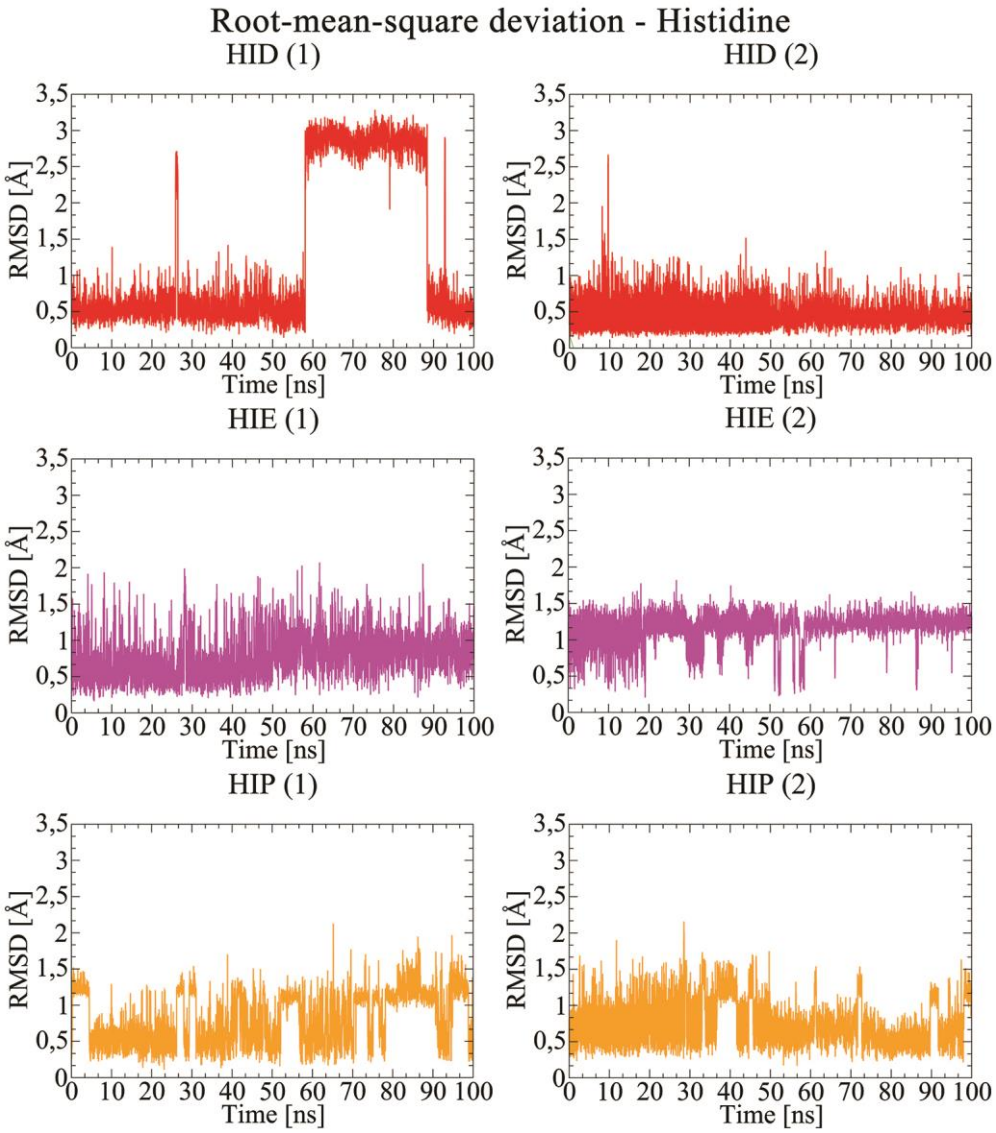

Figure S11: Root-mean-square deviation (RMSD) values for histidine, fitted on the backbone of the protein of the flumazenil-containing simulations.

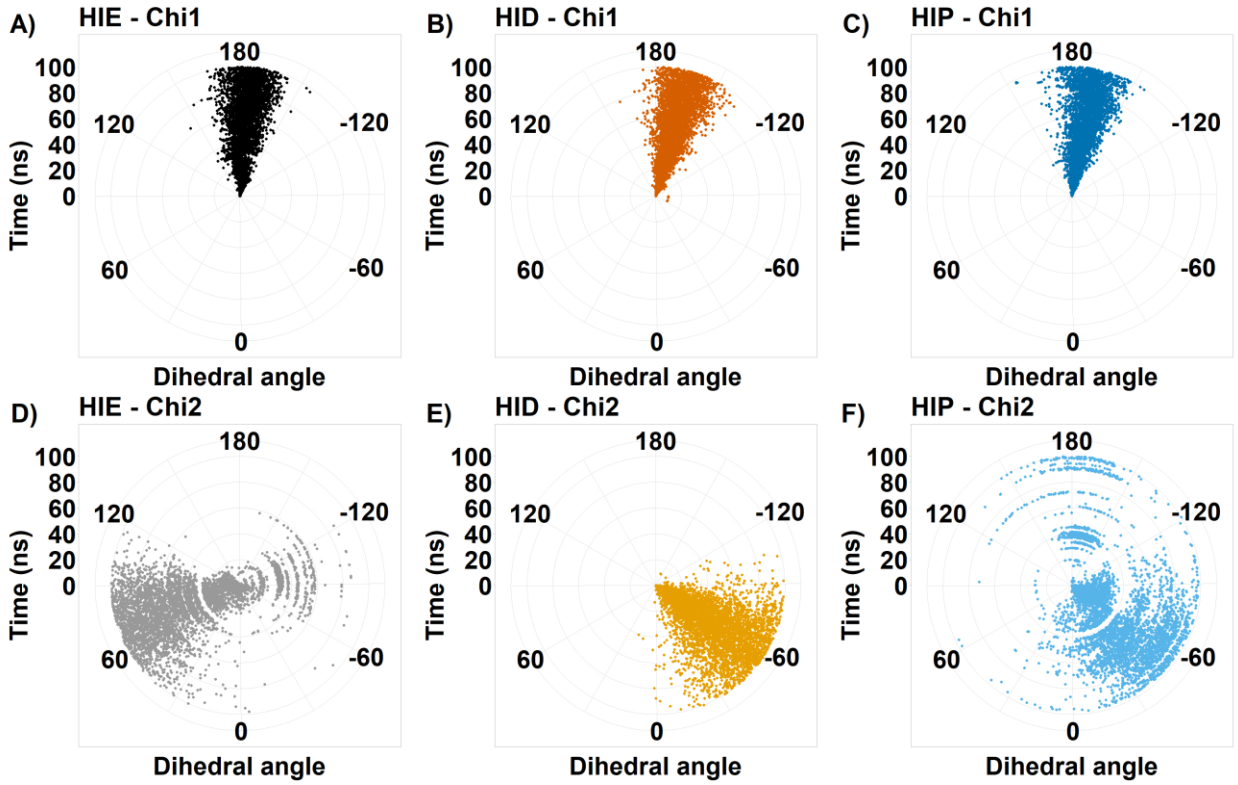

Figure S12: Dihedral distribution for the 100-ns second set of simulations of flumazenil-containing systems. The dihedrals adopted by histidine are similar to those obtained in the other set of trajectories.

Simulations of H102R systems:

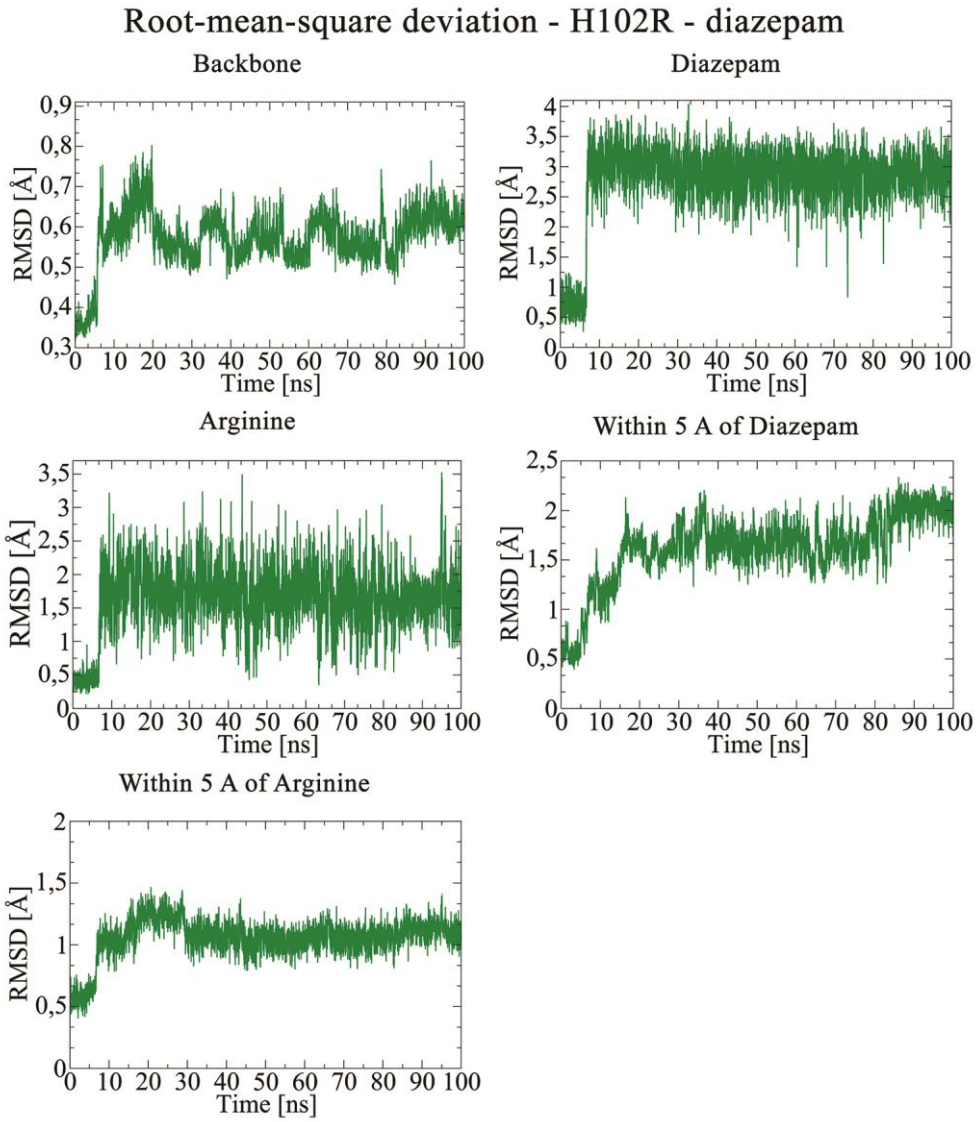

Figure S13: RMSD analysis of the trajectories of the receptor with the H102R mutation in complex with diazepam.

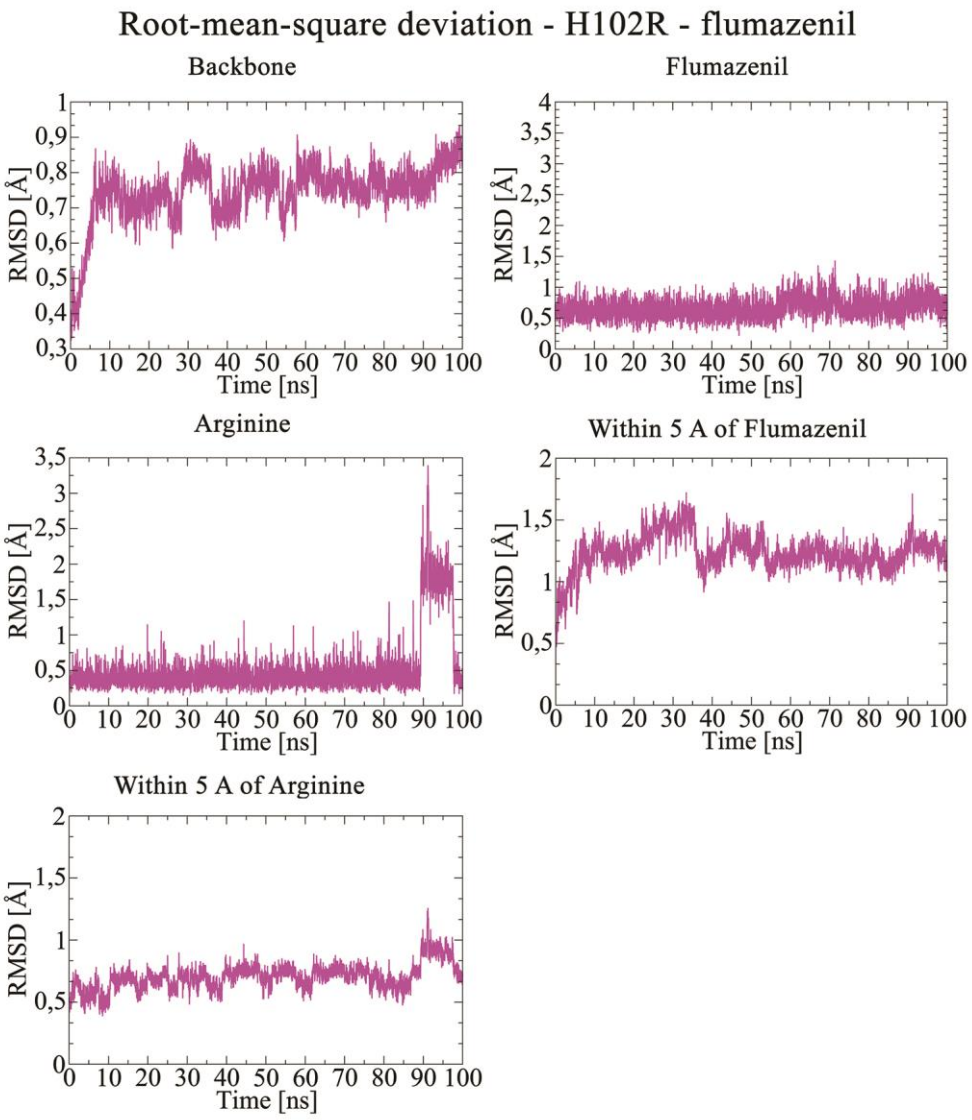

Figure S14: RMSD analysis of the trajectories of the receptor with the H102R mutation in complex with flumazenil.

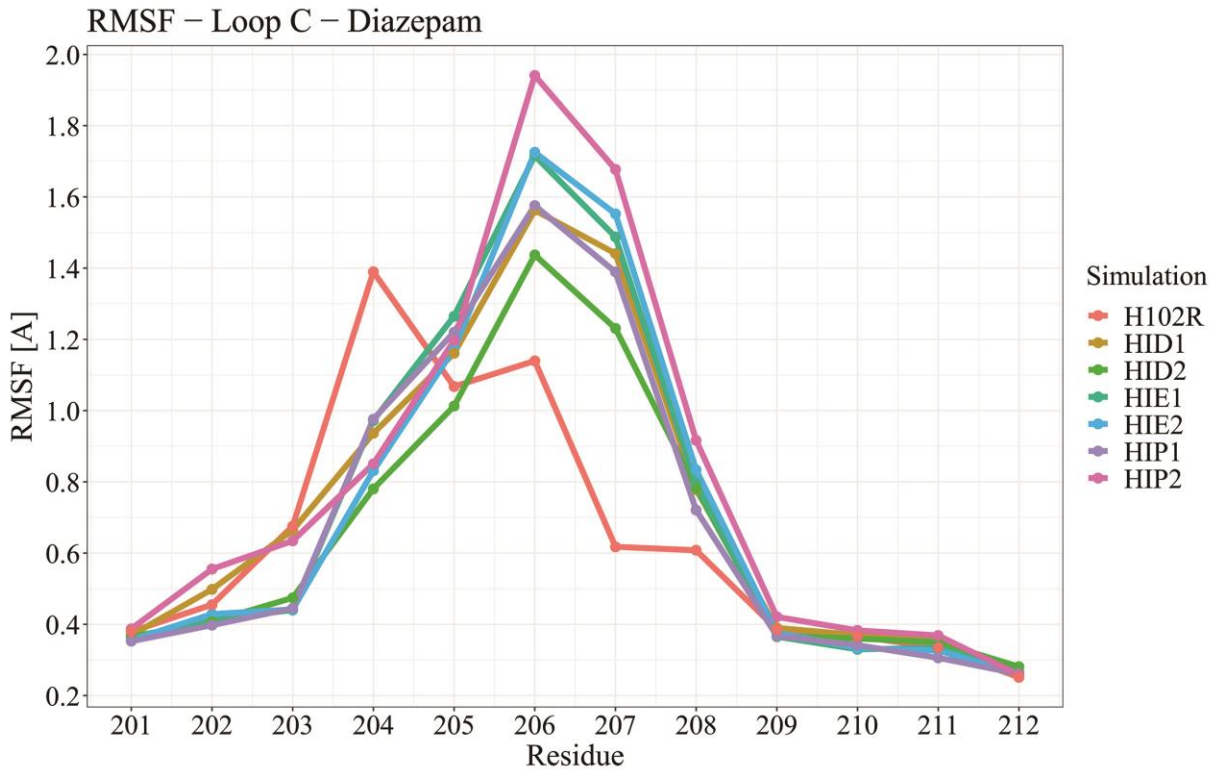

Figure S15: Root-mean-square fluctuation of the Cα atoms of the Loop C residues in the diazepam trajectories.

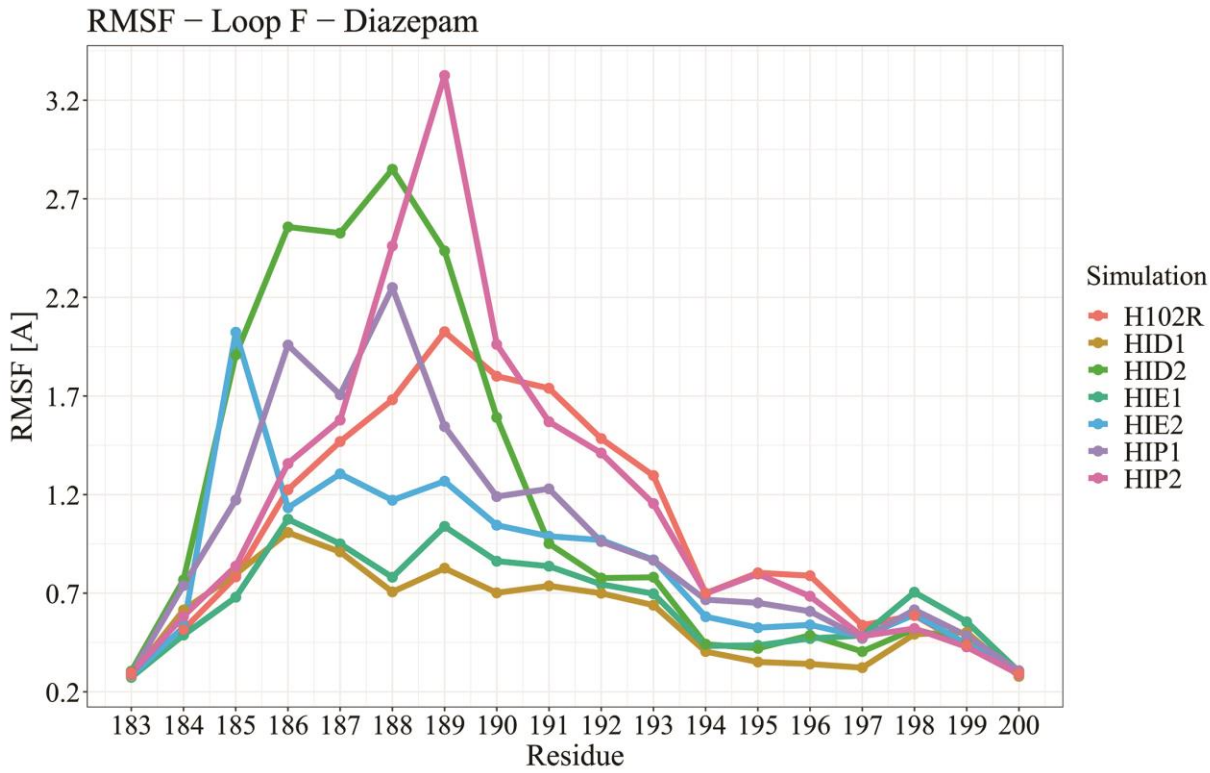

Figure S16: Root-mean-square fluctuation of the Cα atoms of the Loop F residues in the diazepam trajectories.

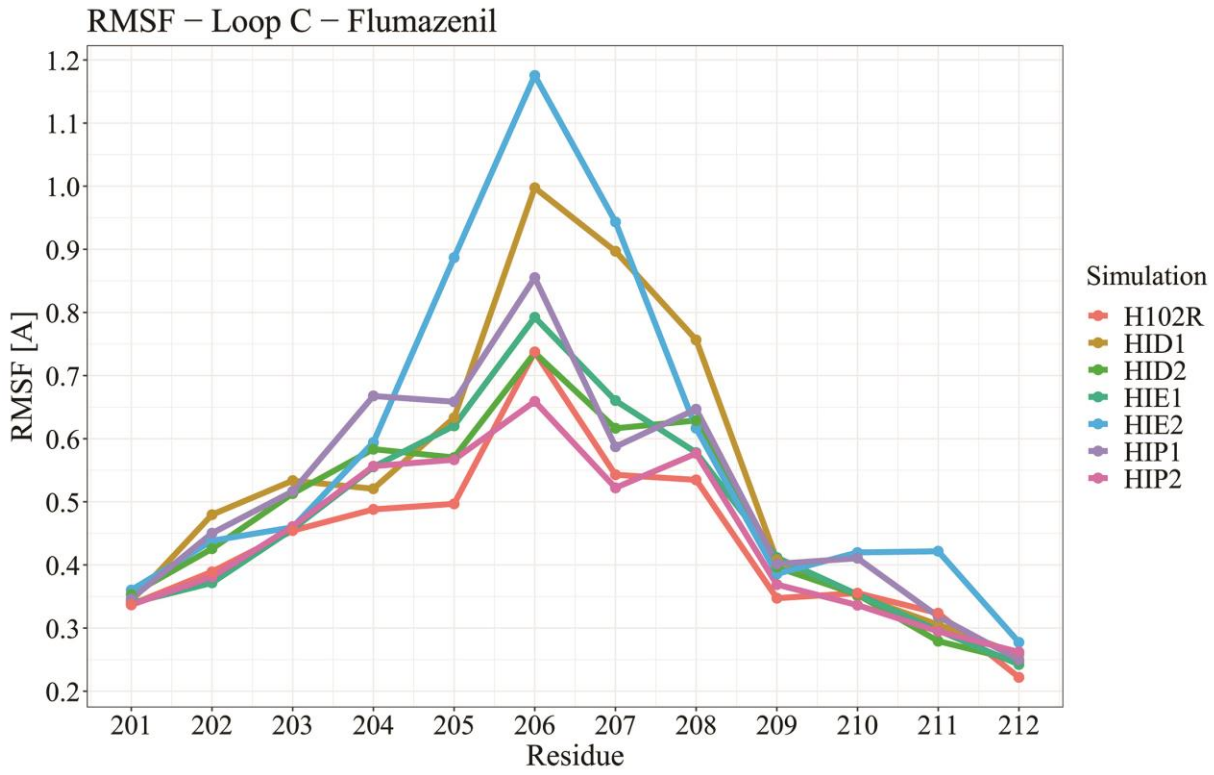

Figure S17: Root-mean-square fluctuation of the Cα of the Loop C in the flumazenil trajectories.

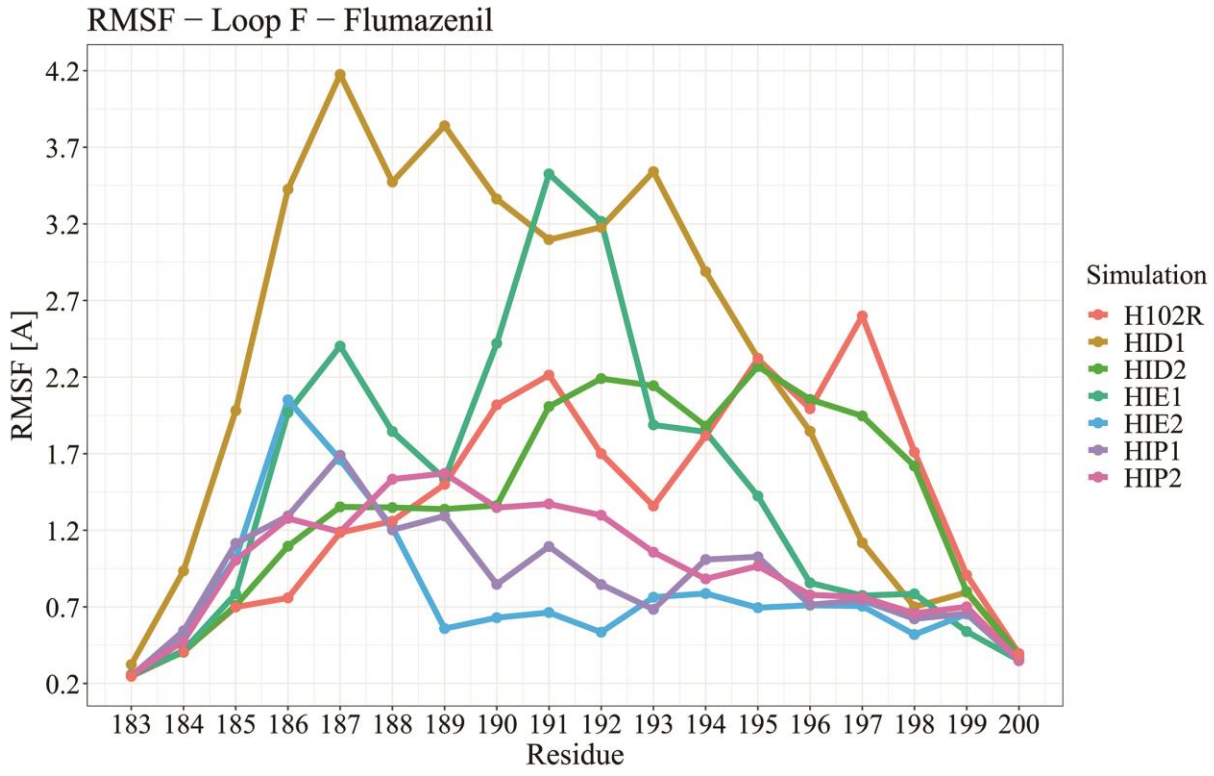

Figure S18: Root-mean-square fluctuation of the Cα of the Loop F in the flumazenil trajectories.

Comparison with cryo-EM structures:

Table S4: Structural comparison of the backbone and diazepam position and orientation, through the RMSD values calculated taking the PDB ID: 6X3X structure as reference and evaluating it through the trajectories of the simulations.

System	RMSD backbone [Å]	RMSD diazepam [Å]
HID1	4.03 ± 0.02	2.3 ± 0.3
HID2	4.01 ± 0.04	2.3 ± 0.3
HIE1	4.03 ± 0.02	2.4 ± 0.2
HIE2	4.03 ± 0.02	2.5 ± 0.3
HIP1	4.02 ± 0.03	2.3 ± 0.3
HIP2	4.01 ± 0.04	2.8 ± 0.7

Table S5: Structural comparison of the backbone and flumazenil position and orientation, through the RMSD values calculated taking the PDB ID: 6X3U structure as reference and evaluating it through the trajectories of the simulations.

System	RMSD backbone [Å]	RMSD flumazenil [Å]
HID1	1.57 ± 0.07	1.3 ± 0.3
HID2	1.50 ± 0.09	0.9 ± 0.2
HIE1	1.58 ± 0.06	1.8 ± 0.5
HIE2	1.51 ± 0.03	4.0 ± 1.6
HIP1	1.52 ± 0.03	1.5 ± 0.7
HIP2	1.75 ± 0.05	1.0 ± 0.2

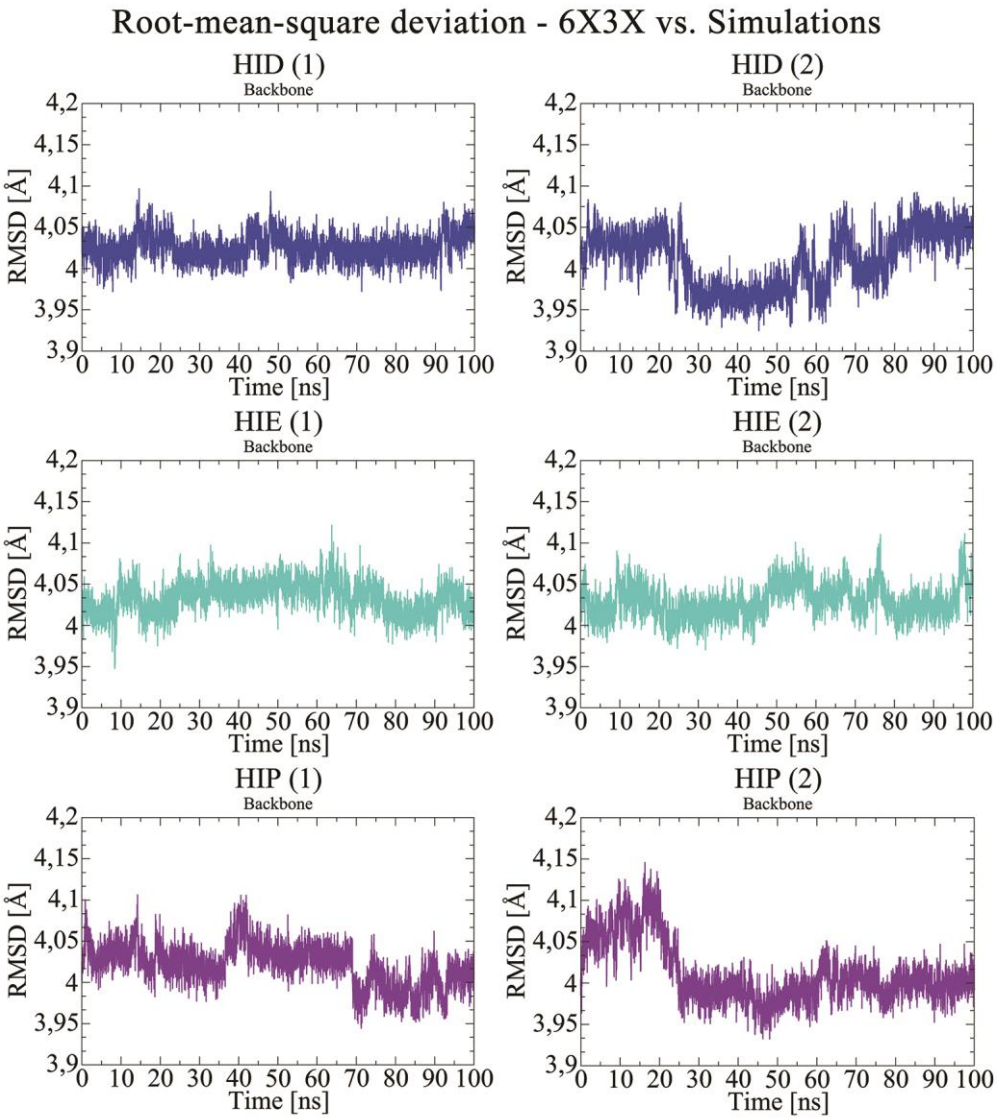

Figure S19: Root-mean-square deviation (RMSD) values for the backbone, fitted on the backbone of the protein PDB ID: 6X3X, of the diazepam-containing simulations.

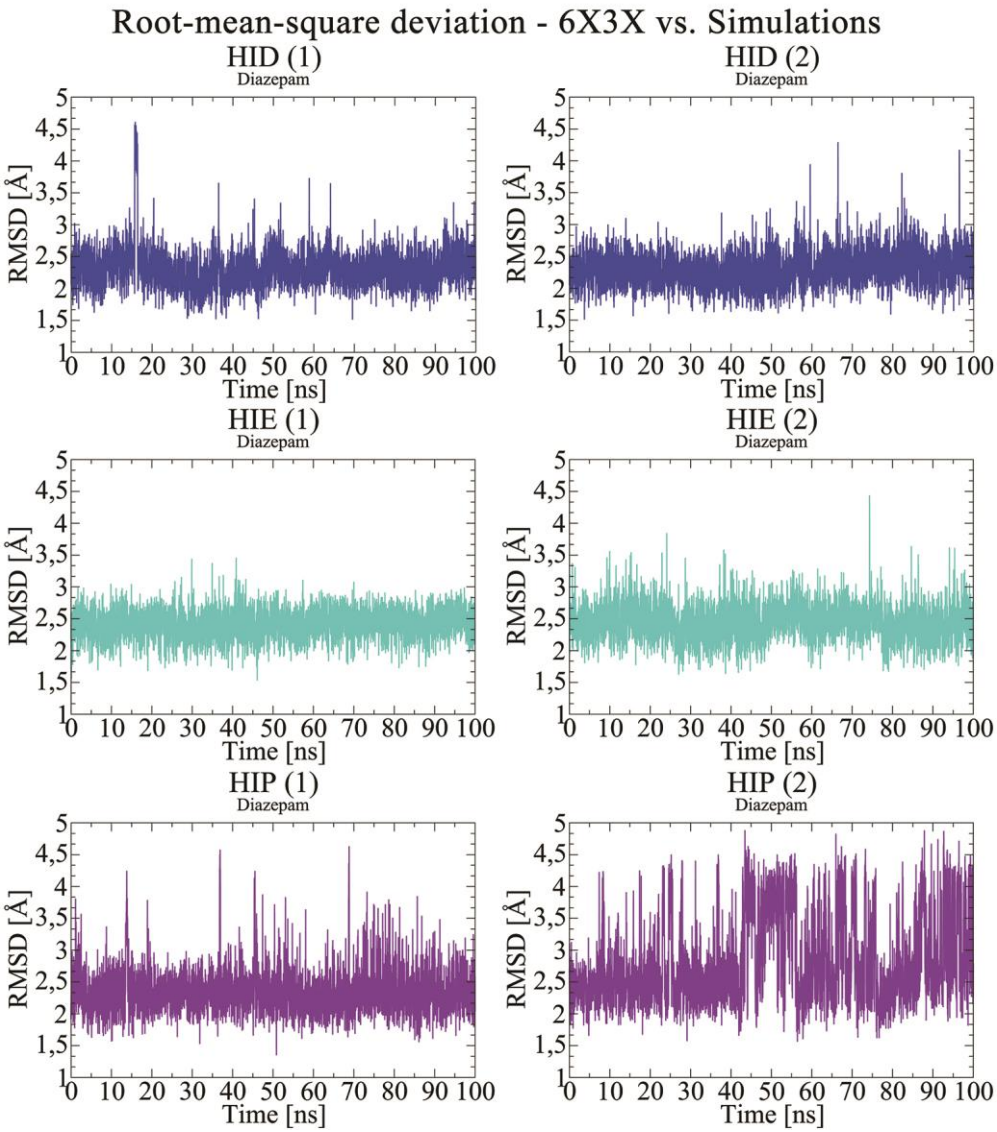

Figure S20: Root-mean-square deviation (RMSD) values for diazepam, fitted on the backbone of the protein PDB ID: 6X3X, of the diazepam-containing simulations.

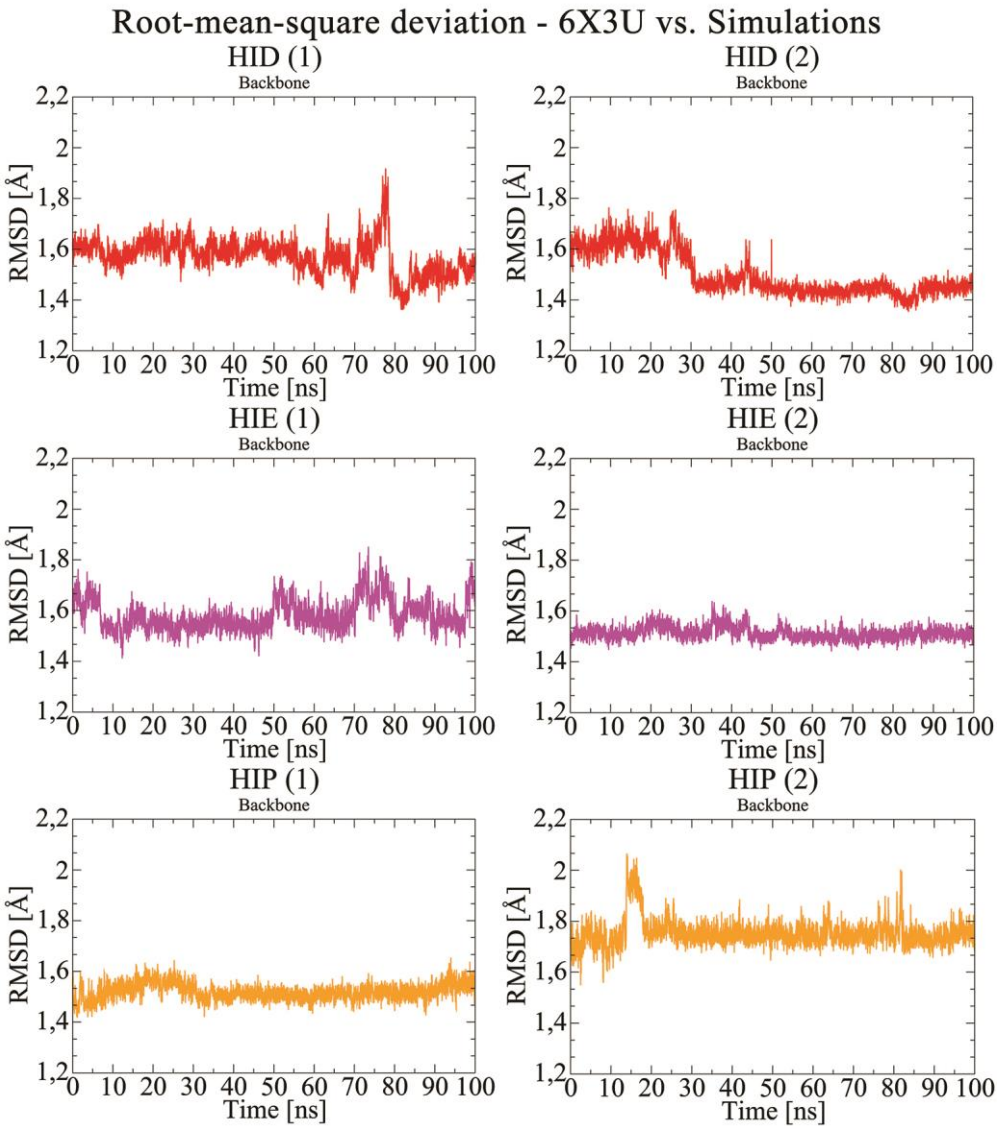

Figure S21: Root-mean-square deviation (RMSD) values for the backbone, fitted on the backbone of the protein PDB ID: 6X3U, of the flumazenil-containing simulations.

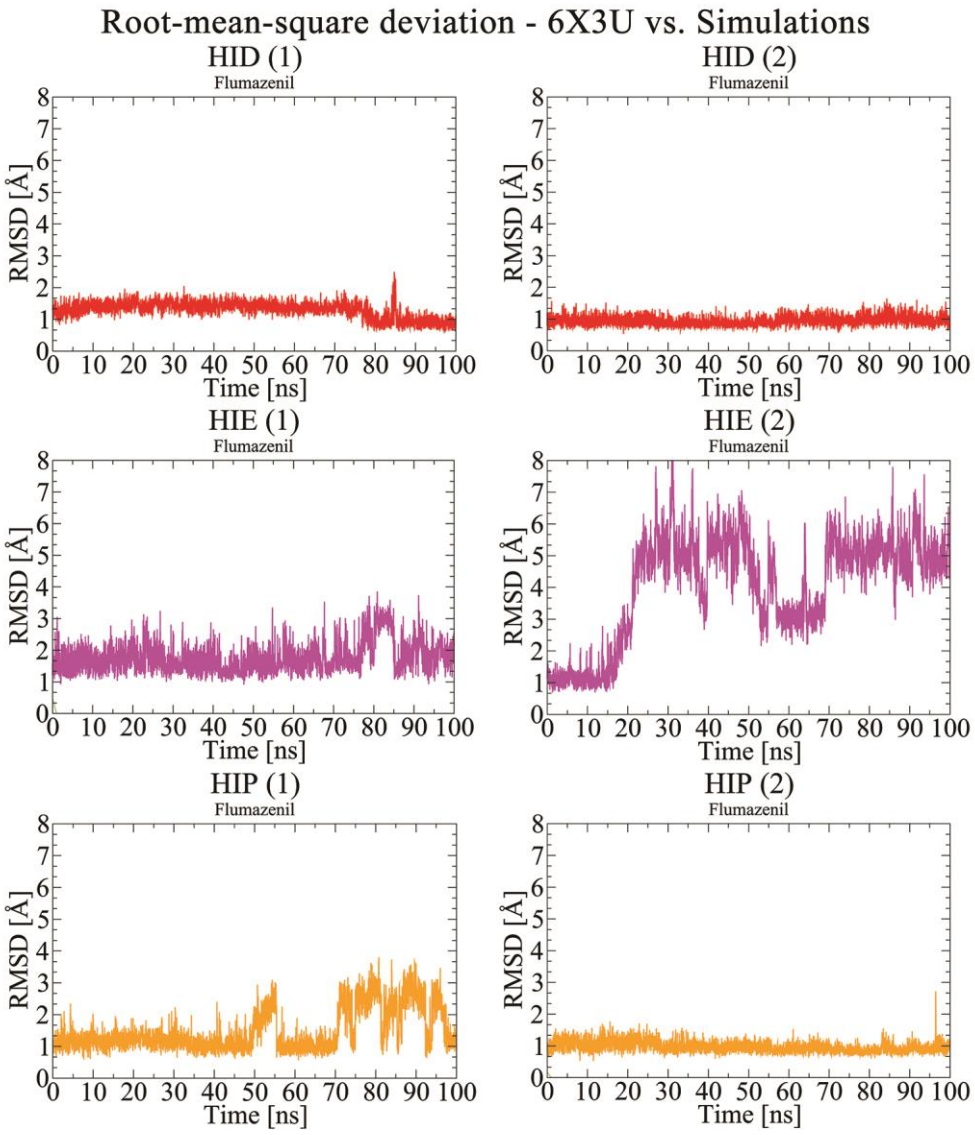

Figure S22: Root-mean-square deviation (RMSD) values for flumazenil, fitted on the backbone of the protein PDB ID: 6X3U, of the flumazenil-containing simulations.

Adaptive biasing force method simulations

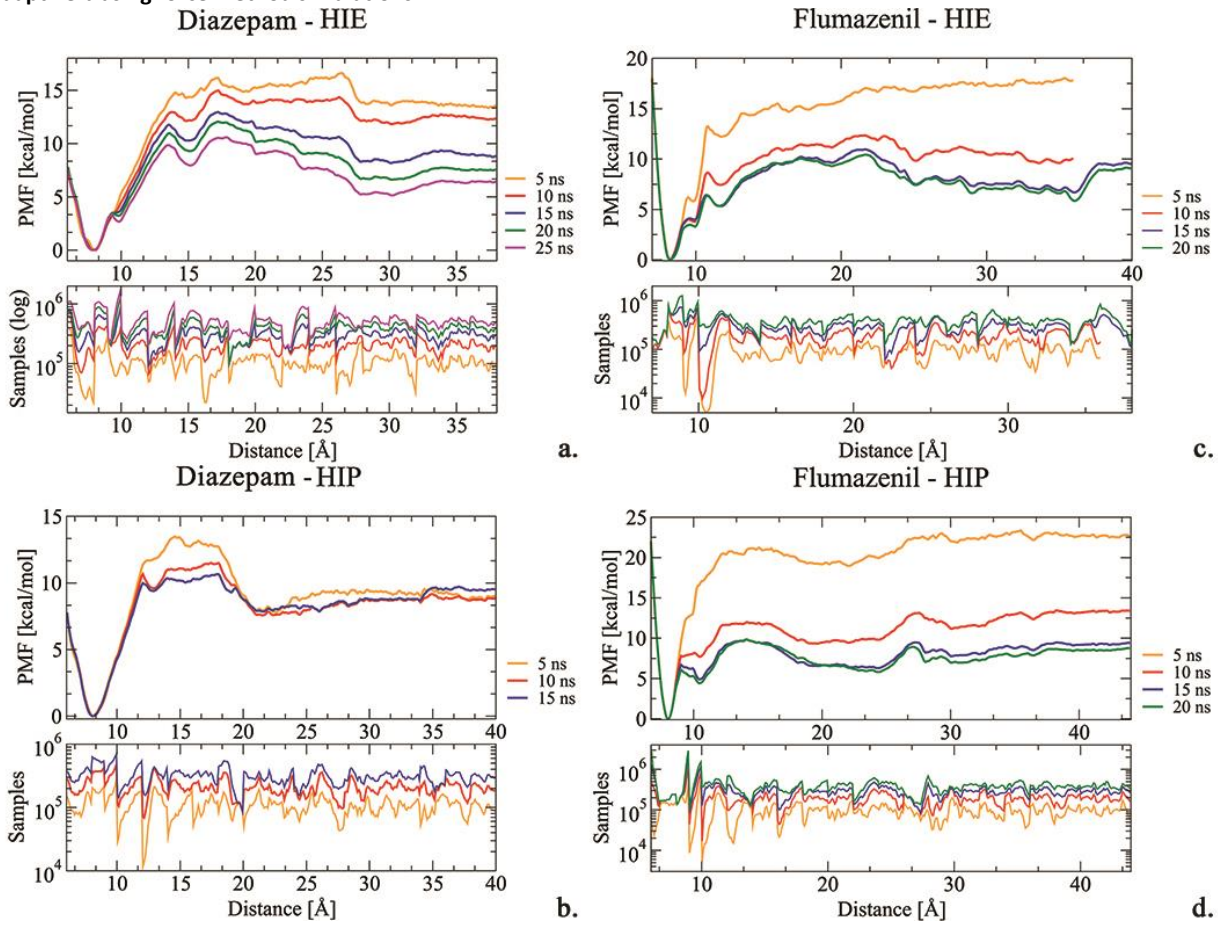

Figure S23: PMF and sampling plots for the ABF simulations of diazepam (a and b) and flumazenil (c and d) in HIE and HIP protonations states.

Table S6: Experimental values for the binding free energy of diazepam to $\alpha_1\beta_2\gamma_2$ $GABA_A$ receptors.

Ki [nM]	ΔG [kcal/mol]	Reference
16.0 ± 0.5	11.1 ± 0.2	[20]
11.0 ± 1.3	11.3 ± 0.7	[21]
14.5 ± 3.7	11.1 ± 1.6	[22]
19.4 ± 0.3	10.9 ± 0.1	[23]
5.4 ± 2.5	11.7 ± 2.9	[24]
16.1 ± 1	11.1 ± 0.4	[25] compiled by [26]
10.3 ± 1.2	11.3 ± 0.7	[26]

Table S7: Experimental values for the binding free energy of flumazenil to $\alpha_1\beta_2\gamma_2$ $GABA_A$ receptors.

Ki [nM]	ΔG [kcal/mol]	Reference
0.5 ± 0.2	13.2 ± 0.3	[20,27]
3.5 ± 0.2	11.99 ± 0.04	[28]
4.3 ± 0.9	11.9 ± 0.1	[29]
1.3 ± 0.1	12.60 ± 0.05	[30]
1.4 ± 0.1	12.56 ± 0.04	[21]
0.7 ± 0.11*	12.98 ± 0.09	[22,31]
0.6 ± 0.1 *	13.1 ± 0.1	[24]

*Kd

References

1. Miller PS, Aricescu AR. Crystal structure of a human GABAA receptor. Nature [Internet]. 2014;512(7514):270–5. Available from: http://dx.doi.org/10.1038/nature13293
2. Pei J, Grishin N V. PROMALS: towards accurate multiple sequence alignments of distantly related proteins. Bioinformatics [Internet]. 2007;23(7):802–8. Available from: +
3. Söding J, Biegert A, Lupas AN. The HHpred interactive server for protein homology detection and structure prediction. Nucleic Acids Res [Internet]. 2005;33($suppl_2$):W244–8. Available from: http://dx.doi.org/10.1093/nar/gki408
4. Arnold K, Bordoli L, Kopp J, Schwede T. The SWISS-MODEL workspace: a web-based environment for protein structure homology modelling. Bioinformatics [Internet]. 2006;22(2):195–201. Available from: +
5. Biasini M, Bienert S, Waterhouse A, Arnold K, Studer G, Schmidt T, et al. SWISS-MODEL: modelling protein tertiary and quaternary structure using evolutionary information. Nucleic Acids Res [Internet]. 2014;42(W1):W252–8. Available from: http://dx.doi.org/10.1093/nar/gku340
6. Bergmann R, Kongsbak K, Sørensen PL, Sander T, Balle T, S??rensen PL, et al. A Unified Model of the GABAA Receptor Comprising Agonist and Benzodiazepine Binding Sites. PLoS One. 2013;8(1):1–13.

7. Sali A. MODELLER: A Program for Protein Structure Modeling Release 9.12, r9480. Rockefeller Univ [Internet]. 2013; Available from: http://scholar.google.com/scholar?hl=en&btnG=Search&q=intitle:MODELLER+A+Program+for+Protein+Structure+Modeling#6

8. Wiederstein M, Sippl MJ. ProSA-web: interactive web service for the recognition of errors in three-dimensional structures of proteins. Nucleic Acids Res [Internet]. 2007;35(suppl_2):W407–10. Available from: http://dx.doi.org/10.1093/nar/gkm290

9. Benkert P, Tosatto SCE, Schomburg D. QMEAN: A comprehensive scoring function for model quality assessment. Proteins. 2008;71(1):261–77.

10. Laskowski RA, MacArthur MW, Moss DS, Thornton JM. PROCHECK: a program to check the stereochemical quality of protein structures. J Appl Crystallogr [Internet]. 1993;26(2):283–91. Available from: https://doi.org/10.1107/S0021889892009944

11. Emsley P, Lohkamp B. Features and development of Coot. 2010;486–501.

12. Søndergaard CR, Olsson MHM, Rostkowski M, Jensen JH. Improved treatment of ligands and coupling effects in empirical calculation and rationalization of p K a values. J Chem Theory Comput. 2011;7(7):2284–95.

13. Olsson MHM, Søndergaard CR, Rostkowski M, Jensen JH. PROPKA3: consistent treatment of internal and surface residues in empirical p K a predictions. J Chem Theory Comput. 2011;7(2):525–37.

14. Dolinsky TJ, Czodrowski P, Li H, Nielsen JE, Jensen JH, Klebe G, et al. PDB2PQR: expanding and upgrading automated preparation of biomolecular structures for molecular simulations. Nucleic Acids Res [Internet]. 2007 Jul [cited 2014 Mar 22];35(Web Server issue):W522-5. Available from: http://www.pubmedcentral.nih.gov/articlerender.fcgi?artid=1933214&tool=pmcentrez&rendertype=abstract

15. Dolinsky TJ, Nielsen JE, McCammon JA, Baker NA. PDB2PQR: An automated pipeline for the setup of Poisson-Boltzmann electrostatics calculations. Nucleic Acids Res. 2004;32(WEB SERVER ISS.):665–7.

16. Trott O, Olson AJ. AutoDock Vina: Improving the speed and accuracy of docking with a new scoring function, efficient optimization, and multithreading. J Comput Chem [Internet]. 2010;31(2):455–61. Available from: http://dx.doi.org/10.1002/jcc.21334

17. Amundarain MJ, Viso JF, Zamarreño F, Giorgetti A, Costabel M. Orthosteric and benzodiazepine cavities of the α1β2γ2 GABAA receptor: insights from experimentally validated in silico methods. J Biomol Struct Dyn [Internet]. 2018;37(6):1597–615. Available from: https://doi.org/10.1080/07391102.2018.1462733

18. Wang J, Wolf RM, Caldwell JW, Kollman PA, Case DA. Development and testing of a general amber force field. J Comput Chem. 2004;25(9):1157–74.

19. Storer JW, Giesen DJ, Cramer CJ, Truhlar DG. Class IV charge models: A new semiempirical approach in quantum chemistry. J Comput Aided Mol Des [Internet]. 1995;9(1):87–110. Available from: https://doi.org/10.1007/BF00117280

20. Pritchett DB, Sontheimer H, Shivers BD, Ymer S, Kettenmann H, Schofield PR, et al. Importance of

a novel GABAA receptor subunit for benzodiazepine pharmacology. Nature. 1989;338(6216):582.

21. Ogris W, Pöltl A, Hauer B, Ernst M, Oberto A, Wulff P, et al. Affinity of various benzodiazepine site ligands in mice with a point mutation in the GABA A receptor γ2 subunit. Biochem Pharmacol. 2004;68(8):1621–9.

22. Baur R, Lüscher BP, Richter L, Sigel E. A residue close to α1 loop F disrupts modulation of GABAA receptors by benzodiazepines while their binding is maintained. J Neurochem. 2010;115(6):1478–85.

23. Davies M, Newell JG, Derry JMC, Martin IL, Dunn SMJ. Characterization of the interaction of zopiclone with $γ$-aminobutyric acid type A receptors. Mol Pharmacol. 2000;58(4):756–62.

24. Berezhnoy D, Nyfeler Y, Gonthier A, Schwob H, Goeldner M, Sigel E. On the benzodiazepine binding pocket in GABAA receptors. J Biol Chem. 2004;279(5):3160–8.

25. Lüddens H, Pritchett DB, Köhler M, Killisch I, Keinänen K, Monyer H, et al. Cerebellar GABAA receptor selective for a behavioural alcohol antagonist. Nature [Internet]. 1990;346(6285):648–51. Available from: https://doi.org/10.1038/346648a0

26. Sieghart W. Structure and Pharmacology of gamma-Aminobotyric AcidA Receptor Subtypes. Pharmacol Rev. 1995;47(2):182–224.

27. Wieland HA, Lüddens H. Four Amino Acid Exchanges Convert a Diazepam-Insensitive, Inverse Agonist-Preferring GABAA Receptor into a Diazepam-Preferring GABAA Receptor. J Med Chem. 1994;37(26):4576–80.

28. Kucken AM, Teissére JA, Seffinga-Clark J, Wagner DA, Czajkowski C. Structural requirements for imidazobenzodiazepine binding to GABAA receptors. Mol Pharmacol. 2003;63(2):289–96.

29. Boileau AJ, Kucken AM, Evers AR, Czajkowski C. Molecular dissection of benzodiazepine binding and allosteric coupling using chimeric γ-aminobutyric acid(A) receptor subunits. Mol Pharmacol. 1998;53(2):295–303.

30. Derry JMC, Dunn SMJ, Davies M. Identification of a residue in the gamma-aminobutyric acid type A receptor a subunit that differentially affects diazepam-sensitive and -insensitive benzodiazepine site binding. J Neurochem. 2004;88:1431–8.

31. Middendorp SJ, Puthenkalam R, Baur R, Ernst M, Sigel E. Accelerated Discovery of Novel Benzodiazepine Ligands by Experiment-Guided Virtual Screening Accelerated Discovery of Novel Benzodiazepine Ligands by Experiment-Guided Virtual Screening University of Bern. ACS Chem Biol. 2014;9:1854–9.